Springer

KSME

Journal of Mechanical Science and Technology 27 (4) (2013) 1031~1039
www.springerlink.com/content/1738-494x
DOI 10.1007/s12206-013-0211-y

Thermal buckling analysis of annular FGM plate having variable thickness under thermal load of arbitrary distribution by finite element method †

Mansour Mohieddin Ghomshei* and Vahid Abbasi

Department of Mechanical Engineering, Islamic Azad University - Karaj Branch, Karaj, Alborz, 31485-313, Iran

(Manuscript Received November 6, 2011; Revised October 9, 2012; Accepted December 25, 2012)

Abstract

In this paper, a finite element formulation is developed for analyzing the axisymmetric thermal buckling of FGM annular plates of variable thickness subjected to thermal loads generally distributed nonuniformly along the plate radial coordinate. The FGM assumed to be isotropic with material properties graded in the thickness direction according to a simple power-law in terms of the plate thickness coordinate, and has symmetry with respect to the plate midplane. At first, the pre-buckling plane elasticity problem is developed and solved using the finite element method, to determine the distribution of the pre-buckling in-plane forces in terms of the temperature rise distribution. Subsequently, based on Kierchhoff plate theory and using the principle of minimum total potential energy, the weak form of the differential equation governing the plate thermal stability is derived, then by employing the finite element method, the stability equations are solved numerically to evaluate the thermal buckling load factor. Convergence and validation of the presented finite element model are investigated by comparing the numerical results with those available in the literature. Parametric studies are carried out to cover the effects of parameters including thickness-to-radius ratio, taper parameter and boundary conditions on the thermal buckling load factor of the plates.

Keywords: Annular plate; FGM; Finite element method; Thermal buckling; Variable thickness

1. Introduction

Functionally graded materials (FGMs) have found important applications especially in aerospace and nuclear industries. The applications include the situations where a structural element has to experience thermal stresses due to a nonuniformly distributed temperature rise. Thermal buckling is an important failure mode in plates and shells. Geometrically perfect plates that are restrained from in-plane expansion when slowly heated generally develop compressive stresses and then buckle at a specific temperature. On the other hand, design of such structural elements with minimum weight is of special interest, particularly in weight sensitive applications, such as aircraft and space vehicles. By an accurate design of thickness distribution, one can get the same required buckling capacity of a plate with considerable weight reduction compared to its uniform thickness counterpart.

Raju and Rao [1] studied the post-buckling behavior of homogenous isotropic circular plates of linearly tapered thickness subject to thermal load by implementing a finite element formulation. They took into account the shear deformation effects in their modeling. Assuming Kierchhoff plate theory and applying the Rayleigh-Ritz method, Ciancio et al. [2] evaluated the buckling behavior of circular and annular plates of continuously variable thickness used as internal bulkheads in submersibles. They assumed an exponential function for the plate thickness variations. Özakça et al. [3] developed a finite element formulation for the buckling analysis of tapered circular and annular plates under mechanical in-plane loads, using an axisymmetric Mindlin-Reissner theory. Najafizadeh and Hedayati [4] presented an analytical solution for axisymmetric thermal and mechanical buckling of functionally graded circular plates of uniform thickness based on first order shear deformation plate theory (FSDPT). They studied the plate buckling under temperature differences of uniform, linear and nonlinear gradient through the thickness. Implementing the exact element method, Efraim and Eisenberger [5] carried out an exact vibration analysis of variable thickness thick annular isotropic and FGM plates based on FSDPT. Jalali et al. [6] analyzed the thermal stability behavior of laminated functionally graded circular sandwich plates of variable thickness, based on the FSDPT, using a pseudo-spectral method. The laminated FGM plate is considered as a sandwich plate constituted of a homogeneous core of variable thickness and two FGM face sheets. Zenkour and Sobhy [7] studied the thermal

*Corresponding author. Tel.: +9826 34418143 5, Fax.: +9826 34418156
E-mail address: ghomshei@kiau.ac.ir
† Recommended by Associate Editor Heung Soo Kim

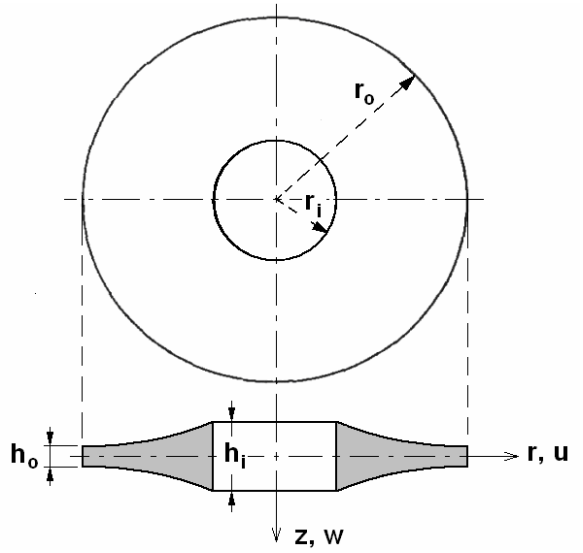

Fig. 1. Geometry of an FGM annular plate of variable thickness, with coordinate axes.

buckling of several kinds of uniform thickness symmetric FGM sandwich plates with a homogeneous isotropic core layer using a sinusoidal shear deformation plate theory. They assumed thermal loads be uniform, linear and non-linear distribution through the thickness.

This work presents a finite element formulation for analyzing the axisymmetric thermal buckling of FGM annular plates of variable thickness under thermal loads having an arbitrary non-uniform distribution through the plate radial coordinate. The FGM assumed to be isotropic with properties graded in the thickness direction according to a simple power-law in terms of the plate thickness coordinate, and has symmetry with respect to the plate midplane. At first, the weak form of the pre-buckling plane elasticity is developed. Next, based on Kierchhoff plate theory and using the principle of minimum total potential energy, the weak form of the differential equation governing the plate thermal stability is derived. Second, using finite element method, the weak form of the plane elasticity is descretized and solved to determine the distribution of the prebuckling inplane forces in terms of the temperature difference. Subsequently, the stability equation is descretized by FEM and solved to evaluate the thermal buckling load factor. Finally, validation and convergence of the present FEM is investigated by comparing the numerical results with a number of published works. Also, parametric studies are conducted to investigate the effects of some important parameters on the thermal buckling load factor of the plates.

2. Theoretical formulation

The geometry of a FGM annular plate of variable thickness is illustrated in Fig. 1 with its profile and selected coordinate axes. The thickness variations as in Ref. [1], is expressed generally by:

$$h = h_i\left[1-\beta\left(\frac{r-r_i}{r_o-r_i}\right)^{\eta}\right] \tag{1}$$

in which η denotes the degree of the thickness variations, and β is a nondimensional parameter defined by:

$$\beta = \frac{h_i - h_o}{h_i} \tag{2}$$

where h_i, h_o are the plate thicknesses at the interior and exterior edges respectively. For a plate of linear thickness variations (η = 1), β is termed taper parameter. A material property, P, such as elastic modulus, E, and coefficient of thermal expansion, α, assumed to vary according to a simple power law along the thickness coordinate z at each side of the plate midplane, and has symmetry with respect to the midplane, which can be expressed as:

$$P^{(1)}(z) = P_m + (P_c - P_m)\left(-\frac{2z}{h(r)}\right)^k, \quad -\frac{h(r)}{2} \le z \le 0$$
$$P^{(2)}(z) = P_m + (P_c - P_m)\left(\frac{2z}{h(r)}\right)^k, \quad 0 \le z \le \frac{h(r)}{2} \tag{3}$$

where P_m, P_c are properties of metal and ceramic respectively, $h(r)$ is the plate thickness at the radial position r, and k is the volume fraction index. In this study, however Poisson's ratio, ν, which has small variations, is considered as a constant.

In order to determine the pre-buckling membrane force distribution due to temperature rise in the annular plate, under axisymmetric conditions, here we develop the pre-buckling plane elasticity problem. Stating the static equilibrium equation along radial direction for an element of the plate in polar coordinate, we obtain:

$$\frac{dN_r}{dr} + \frac{N_r - N_\theta}{r} = 0 \tag{4}$$

where N_r, N_θ are inplane radial and peripheral forces per unit length respectively. Solving the equation for N_θ, results in:

$$N_\theta = \frac{d}{dr}(rN_r)\,. \tag{5}$$

The plate constitutive equation in plane elasticity can be written as:

$$\begin{Bmatrix} N_r \\ N_\theta \\ 0 \end{Bmatrix} = [A]\begin{Bmatrix} \varepsilon_r^0 \\ \varepsilon_\theta^0 \\ 0 \end{Bmatrix} - \begin{Bmatrix} N_r^T \\ N_\theta^T \\ 0 \end{Bmatrix} \tag{6}$$

where $[A]$ is the extensional stiffness, ε_r^0, ε_θ^0 are the radial

and peripheral strains respectively, and N_r^T, N_θ^T denote the thermal forces per unit length. The strains in terms of radial displacement, u_0, can be obtained as [8]:

$$\varepsilon_r^0 = \frac{du_0}{dr}, \quad \varepsilon_\theta^0 = \frac{u_0}{r}, \quad \gamma_{r\theta}^0 = 0 \tag{7}$$

and, the thermal forces are calculated by [8]:

$$N_r^T = N_\theta^T = \frac{\Delta T(r)}{1-\nu} \int_{-\frac{h(r)}{2}}^{\frac{h(r)}{2}} E(z)\alpha(z)dz \,. \tag{8}$$

By substituting from Eq. (3) for $E(z)$ and $\alpha(z)$, into the above equation, and performing the integration, we obtain:

$$N_r^T = \frac{F\, h(r)\Delta T(r)}{1-\nu} \tag{9}$$

where

$$F = E_m\alpha_m + \frac{E_m\alpha_c - 2E_m\alpha_m + E_c\alpha_m}{k+1} + \frac{E_c\alpha_c - E_c\alpha_m - E_m\alpha_c + E_m\alpha_m}{2k+1} \,. \tag{10}$$

Substituting from Eq. (7) into Eq. (6), then in the equilibrium Eq. (5), and after some mathematical manipulations, yields the following differential equation in terms of radial displacement u_0:

$$\frac{d}{dr}\left(rA_{11}\frac{du_0}{dr}\right) + \left(\nu\frac{dA_{11}}{dr} - \frac{A_{11}}{r}\right)u_0 - r\frac{dN_r^T}{dr} = 0 \,. \tag{11}$$

This second order differential equation often termed as membrane equation, should be solved with two boundary conditions at the inner and outer edges of the annular plate. At a free edge the boundary condition is $du_0/dr = 0$, and at a fixed end is $u_0 = 0$. The weak form of the differential equation, as it is useful to derive the finite element formulation for the plate prebuckling behavior is as follows:

$$\int_{r_i}^{r_o}\left(a(r)\frac{du_0}{dr}\frac{d\delta u_0}{dr} + C(r)u_0\,\delta u_0 - \delta u_0\, q(r)\right)dr - \delta u_0(r_i)Q_A - \delta u_0(r_o)Q_B = 0 \tag{12}$$

where:

$$a(r) = rA_{11}, \quad C(r) = \frac{A_{11}}{r} - \frac{dA_{12}}{dr}, \quad q(r) = -r\frac{dN_r^T}{dr},$$
$$-Q_A = a(r)\frac{du_0}{dr}\bigg|_{r_i}, \quad Q_B = a(r)\frac{du_0}{dr}\bigg|_{r_o} \,. \tag{13}$$

Now, in order to derive the equation governing the buckling behavior of the plate, we make use of the principle of minimum total potential energy (PMPE). The strain energy stored in the FGM annular plate, due to bending during the thermal buckling, can be obtained by [9]:

$$U = \frac{1}{2}\iiint \left[\sigma\right]^T\left[\varepsilon - \alpha(z)\Delta T(r)\right]rdrd\theta\, dz \tag{14}$$

in that, the strain components in terms of midplane strains and curvatures are stated as [9]:

$$\begin{Bmatrix}\varepsilon_r\\ \varepsilon_\theta\\ \gamma_{r\theta}\end{Bmatrix} = \begin{Bmatrix}\varepsilon_r^0\\ \varepsilon_\theta^0\\ \gamma_{r\theta}^0\end{Bmatrix} + z\begin{Bmatrix}\kappa_r\\ \kappa_\theta\\ \kappa_{r\theta}\end{Bmatrix} \tag{15}$$

where midplane strains $\varepsilon_r^0, \varepsilon_\theta^0, \gamma_{r\theta}^0$ and curvatures $\kappa_r, \kappa_\theta, \kappa_{r\theta}$ in terms of radial and lateral displacements u_0, w are:

$$\varepsilon_r^0 = \frac{du_0}{dr} + \frac{1}{2}\left(\frac{dw}{dr}\right)^2, \quad \varepsilon_\theta^0 = \frac{u_0}{r}, \quad \gamma_{r\theta}^0 = 0,$$
$$\kappa_r = -\left(\frac{d^2w}{dr^2}\right), \quad \kappa_\theta = -\frac{1}{r}\left(\frac{dw}{dr}\right), \quad \kappa_{r\theta} = 0 \,. \tag{16}$$

The stress components are expressed in terms of the strain components by the following constitutive equations, which are the Hook's law:

$$\sigma_r = \frac{E(z)}{(1-\nu^2)}\left[\varepsilon_r + \nu\varepsilon_\theta - (1+\nu)\alpha(z)\Delta T(r)\right]$$
$$\sigma_\theta = \frac{E(z)}{(1-\nu^2)}\left[\varepsilon_\theta + \nu\varepsilon_r - (1+\nu)\alpha(z)\Delta T(r)\right] \tag{17}$$
$$\tau_{r\theta} = \frac{E(z)}{2(1+\nu)}\gamma_{r\theta} \,.$$

By substituting from Eqs. (15)-(17), into Eq. (14), and performing the integrations over z and θ, we obtain:

$$U = \pi\int_{r_i}^{r_o}\begin{bmatrix}\frac{d^2w}{dr^2} & \frac{1}{r}\frac{dw}{dr}\end{bmatrix}\begin{bmatrix}D & \nu D\\ \nu D & D\end{bmatrix}\begin{Bmatrix}\frac{d^2w}{dr^2}\\ \frac{1}{r}\frac{dw}{dr}\end{Bmatrix}r\,dr + \frac{2\pi P}{(1-\nu)}\int_{r_i}^{r_o}h(r)\Delta T^2(r)rdr \tag{18}$$

in that $D = D_{11}$ is the plate flexural rigidity determined by:

$$D = \int_{-\frac{h(r)}{2}}^{\frac{h(r)}{2}}\frac{E(z)z^2}{1-\nu^2}dz = \frac{(3E_c + E_mk)}{12(1-\nu^2)(k+3)}h^3(r) \,. \tag{19}$$

In deriving Eq. (18), midplane strains are neglected, regarding that we should calculate only the strain energy due to bending during the buckling phenomenon. During the plate buckling, the work done by the resultant inplane forces are calculated by the following integral:

$$W = \pi \int_{r_i}^{r_o} N_r \left(\frac{dw}{dr} \right)^2 r\, dr \,. \tag{20}$$

Now, substituting from Eqs. (18) and (20) into the PMPE ($\delta\Pi = \delta U - \delta W = 0$), the weak form of the differential equation governing the plate thermal buckling behavior obtained as the following:

$$\delta\Pi = \int_{r_i}^{r_o} \begin{bmatrix} \frac{d^2 w}{dr^2} & \frac{1}{r}\frac{dw}{dr} \end{bmatrix} \begin{bmatrix} D & \nu D \\ \nu D & D \end{bmatrix} \begin{Bmatrix} \frac{d^2 \delta w}{dr^2} \\ \frac{1}{r}\frac{d\delta w}{dr} \end{Bmatrix} r\, dr - 2\int_{r_i}^{r_o} N_r \left(\frac{dw}{dr} \right) \left(\frac{d\delta w}{dr} \right) r dr = 0 \,. \tag{21}$$

The weak form together with the boundary conditions should be solved to obtain the lateral deflection of the plate. The boundary conditions at a clamped edge is $w = dw/dr = 0$, at a simply supported edge is $w = M_r = 0$, and at a free edge is $M_r = V_r = 0$ in that V_r is the effective shear force.

3. Finite element formulation

Since the equations governing the prebuckling and buckling behaviors of the variable thickness FGM annular plates are differential or variational equations with variable coefficients, in general there are no analytical solutions for them. In this section, finite element approximations for both prebuckling and buckling behaviors are derived. The total domain of the annular plate is divided into axisymmetric elements of equal radial lengths as shown in Fig. 2.

In order to derive the finite element formulation for the plate prebuckling behavior, we make use of the weak form Eq. (12) stated for a typical element in membrane deformation. Each element of this type consists of two nodes, with one degree of freedom per each nod, as shown in Fig. 3. ξ is an element local coordinate, and L is the length of an assumed element. Implementing the Lagrange linear interpolation functions, the element radial displacement function, u^e, can be approximated by [10]:

$$U^e(\xi) \approx u_0^e = N_1 u_{01}^e + N_2 u_{02}^e \tag{22}$$

where, the shape functions N_1^e, N_2^e are defined as:

$$N_1 = (1 - \xi / L), \quad N_2 = (\xi / L) \,. \tag{23}$$

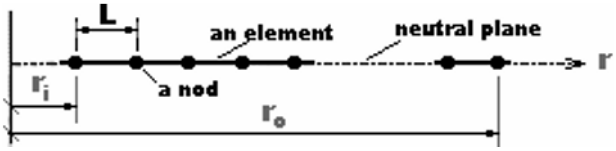

Fig. 2. A schematic diagram showing the nodes and elements included in the problem domain.

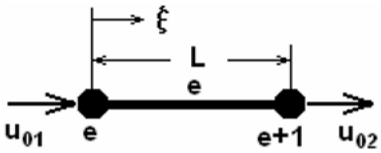

Fig. 3. An element with its nodal degrees of freedom in membrane deformation.

Following the Rayleigh-Ritz procedure, we substitute the approximation function defined by Eq. (22) for u_0, and N_1^e, N_2^e for δu_0 into the weak form Eq. (12) stated for a typical element, then perform the integrations, to obtain the finite element formulation of the prebuckling displacement field as follows:

$$\left[K^e \right] \left\{ u_0^e \right\} = \left\{ f^e \right\} + \left\{ Q^e \right\} \tag{24}$$

where the entries of the stiffness matrix $[K^e]$, force vectors $\{f^e\}$ and $\{Q^e\}$ are determined by:

$$K_{ij}^e = \int_0^L \left\{ a(\xi) \frac{dN_i^e}{d\xi} \left(\sum_{j=1}^{2} \frac{dN_j^e}{d\xi} u_{0j}^e \right) + C(\xi) N_i^e \left(\sum_{j=1}^{2} N_j^e u_{0j}^e \right) \right\} dr$$

$$f_i = \int_0^L \left\{ N_i^e\, q(\xi) \right\} dr, \qquad Q_i^e = \sum_{j=1}^{2} N_i^e(\xi_j^e) Q_j \,. \tag{25}$$

It should be mentioned that the force vector $\{f^e\}$ arises from the radial thermal stresses, and the force vector $\{Q^e\}$ is due to axisymmetric external radial loads which may be applied on the plate. After expanding Eq. (24) to the whole elements in the solution domain and then imposing the plate boundary conditions, the resulting set of linear algebraic equations are to be solved to obtain the displacement vector $\{u_0\}$ as function of the temperature index T_0. Note that $T(r)$ is expressible as $T_0 \times f(r)$. Then, using Eqs. (6) and (7) subsequently, the membrane forces will be determined.

To derive a finite element model for the plate stability equation, we apply the weak form given by Eq. (21) stated for a typical element. The equation is of second order, so we must save deflection and slope data for each nod. An element with its nodal degrees of freedom in transverse deflection is shown in Fig. 4. The approximation of the primary variables over a finite element should be such that it satisfies the essential boundary conditions of the element. So, we make use of Hermite family of interpolation functions to approximate the element displacement function w^e, as [10]:

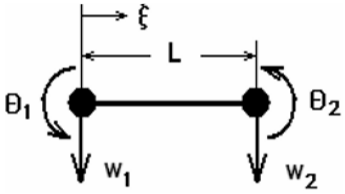

Fig. 4. An element with its nodal degrees of freedom in transverse deflection.

$$w^e(\xi)=\left[\phi_1^e \;\; \phi_2^e \;\; \phi_3^e \;\; \phi_4^e\right]\begin{Bmatrix} w_1 \\ \theta_1 \\ w_2 \\ \theta_2 \end{Bmatrix}=[\Phi^e]\{W^e\} \tag{26}$$

with the shape functions ϕ_i^e defined by:

$$\phi_1^e=1-3\left(\frac{\xi}{L}\right)^2+2\left(\frac{\xi}{L}\right)^3,\quad \phi_2^e=-\xi+2\left(\frac{\xi^2}{L}\right)-\left(\frac{\xi^3}{L^2}\right)$$
$$\phi_3^e=3\left(\frac{\xi}{L}\right)^2-2\left(\frac{\xi}{L}\right)^3,\quad \phi_4^e=\left(\frac{\xi^2}{L}\right)-\left(\frac{\xi^3}{L^2}\right). \tag{27}$$

Substituting from Eq. (26) for w, and each of the shape functions for δw into the weak form of the stability equation (21) stated for an element, then performing the integrations, we obtain the discretized form of the plate stability equation as follows:

$$[k^e]\{W^e\}-[b^e]\{W^e\}=0 \tag{28}$$

in which $[k^e]$, $[b^e]$ are the element elastic stiffness and geometric stiffness matrices respectively, which their entries are determined by the following integrals:

$$k_{ij}^e=\int_0^L\begin{bmatrix}\dfrac{d^2\phi_i^e}{d\xi^2} & \dfrac{1}{r}\dfrac{d\phi_i^e}{d\xi}\end{bmatrix}\begin{bmatrix} D & \nu D \\ \nu D & D\end{bmatrix}\begin{Bmatrix}\dfrac{d^2\phi_j^e}{d\xi^2} \\ \dfrac{1}{r}\dfrac{d\phi_j^e}{d\xi}\end{Bmatrix} r\,d\xi$$
$$b_{ij}^e=2\int_0^L N_r\frac{d\phi_i^e}{d\xi}\frac{d\phi_j^e}{d\xi}r\,d\xi \tag{29}$$

where $r=R_i^e+\xi$, with R_i^e as the radial coordinate of the element internal node. After expanding Eq. (28) to the structure size, then imposing the plate boundary conditions, we obtain:

$$\left[K\right]\{\tilde{W}\}-\left[B\right]\{\tilde{W}\}=0 \tag{30}$$

where [K], [B] are the global elastic stiffness and geometric stiffness matrices respectively, and $\{\tilde{W}\}$ is the generalized vector of nodal displacements, defined as:

Table 1. Material properties of metal and ceramic in the FGM plate.

Materials	Young's modulus	Thermal expansion coeff. (1/°C)	Poisson's ratio (--)
Aluminum	70	23e-6	0.3
Zirconia	380	7.4e-6	0.3

$$\{\tilde{W}\}=[w_1\;\;\theta_1\;\;w_2\;\;\theta_2\;\;\ldots\;\;w_n\;\;\theta_n]^T. \tag{31}$$

In the second of the above Eq. (29), N_r is the radial membrane force which has been found previously by solving the discrete form of the membrane equation, Eq. (24), as a function of the radial coordinate r, multiplied by the temperature rise index T_0, i.e.:

$$N_r=T_0\overline{N}(r). \tag{32}$$

Substituting from Eq. (32) into the second of Eq. (29), the global geometric stiffness may be rewritten as $[B]=T_0[B']$. So, Eq. (30) takes the form:

$$\left[K\right]\{\tilde{W}\}-T_0\left[B'\right]\{\tilde{W}\}=0 \tag{33}$$

or:

$$\left[B'\right]^{-1}\left[K\right]\{\tilde{W}\}=T_0\{\tilde{W}\}. \tag{34}$$

The recent equation is an eigenvalue problem, which can be solved to obtain the critical values of the temperature index T_{0cr} as the eigenvalues, and the mode shapes of buckling as the eigenvectors.

4. Numerical results and discussion

In this section, the numerical results of the thermal buckling of circular and annular FGM plates having constant or variable thicknesses under uniform or nonuniform temperature fields are presented. The solution convergence of the presented finite element formulation is investigated. Also, the F.E. model is validated by comparing its numerical results with those existing in the literature. Parametric studies are conducted to cover the effects of a number of important parameters on the critical thermal buckling of the annular plates. In these computations the FGM plate assumed to be made from a mixture of metal and ceramic whose material properties are as listed in Table 1, unless otherwise specified.

4.1 Convergence of presented FEM formulation

In any finite element model, errors caused by discretization arise, which include the errors due to approximate interpolation functions, as well as those of the numerical integrations. The convergence of the present FEM has been investigated for a simply supported annular homogeneous plate with linearly

Table 2. Comparison of the present buckling load factor λ_T with the results reported in references for circular clamped plates of constant thickness.

	h/r_0 = 0.001	0.01	0.05	0.1	0.2
Present	14.6819	14.6819	14.6819	14.6819	14.6819
Ref. [1]	14.6825	-	14.5299	14.0910	12.5725
Ref. [3]	14.6819	14.6746	14.5014	13.9885	12.2843
Ref. [4]	14.6800	14.6800	14.6800	14.6800	14.6800
Ref. [6]	14.6819	14.6758	14.5296	14.0909	12.5724
Ref. [8]	14.6842	14.6842	14.6842	14.6842	14.6842

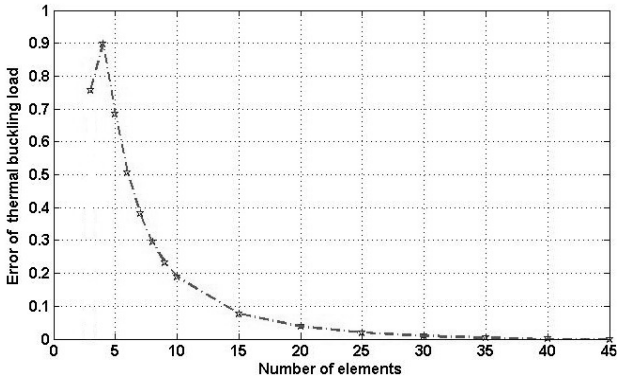

Fig. 5. Convergence of the presented FEM solution with increase in the number of elements.

increasing thickness from center to the outer boundary, subject to a uniform temperature rise. Fig. 5 demonstrates the effect of the number of elements in the problem domain on the normalized error. Selection of the larger number of elements results in the higher accuracy of the results. However, the normalized error descended relatively fast with increase in the number of elements.

4.2 Verification of presented FEM formulation

Since there are comparable submitted results only for homogenous plates, the problem is solved for two cases of homogenous plates, and compared with the existing results in the literature. For this purpose, the volume fraction index k is equated to zero. In Table 2, the values of the critical thermal buckling load factor obtained from the presented analysis along with those reported in Refs. [1, 3, 4, 6] and [8] are presented for the case of a homogenous full ceramic circular plate of constant thickness under a uniform temperature rise, and clamped at exterior edge. The results are presented for five different thickness-to-radius ratios, h/r_0. Thermal buckling load factor, λ_T, is defined as [1]:

$$\lambda_T = 12(1+\nu)T_{0cr}\left(r_0/h\right)^2 . \tag{35}$$

As can be seen in Table 2, there is good agreement between the results of the present analysis with those reported in the

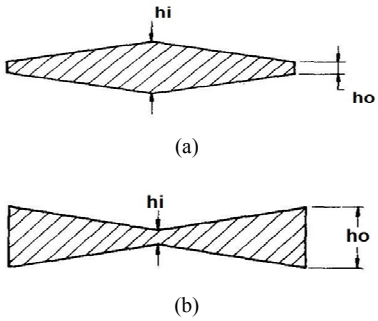

Fig. 6. Profile of a circular plate with linear thickness variations for (a) $\beta > 0$; (b) $\beta < 0$.

references, particularly those associated with the smaller values of h/r_0. This can be explained in this way that, the present FEM analysis is based on the Kierchhoff plate theory which has more accuracy for thin plates, while in the works reported in Refs. [1, 3] and [6] the shear deformation theories are implemented for their analysis.

Thermal buckling of homogenous circular plates with linear variations in their thickness, and simply supported at their edges are studied as the second case. In Fig. 6 the profiles of such plates are illustrated for a positive and a negative value of the taper parameter, i.e. for $\beta > 0$ and $\beta < 0$ respectively. The numerical values of the thermal buckling load factor obtained from the presented FEM, along with those reported in Refs. [1] and [6] are summarized in Table 3, sorted for 9 different values of β, and 4 different values of h_i/r_o. Again, the thermal buckling factor is defined by Eq. (35), in that h is to be replaced by h_i. As mentioned previously, in Refs. [1] and [6] shear deformation is regarded, while the present FEM is based on the thin plate assumptions, and therefore, for smaller values of h_i/r_o, the FEM results have more correspondence with those reported in the references.

It should be mentioned that, since there were no experimental data available, either published or from current work, the results of the present FEM are just compared to those of some other analytical/numerical models which were available in the literature, as summarized in Tables 2 and 3.

4.3 Parametric studies

In this subsection, the effects of a number of parameters on the thermal buckling load factor of the annular plates are studied. In Fig. 7 the critical buckling temperature index, T_{0cr}, is plotted versus the volume fraction index, k, for uniform thickness annular plates of $h/r_o = 0.2$, and $r_i/r_o = 2$, under a uniform thermal load ($T(r) = T_0$). The results are plotted for two different kinds of supporting, a clamped at inner and outer edges (C-C) and a simply supported at both edges (S-S). The value of T_{0cr} decreases as k increases for both kinds of supporting. This can be explained by noting that, as k increments, the volume percent of ceramic in FGM decreases, and as a result the plate bending stiffness decreases, regarding that the metal

Table 3. Comparisons of the present buckling load factor λ_T for a homogenous circular simply-supported plate of linear thickness variations under a uniform thermal load.

		β								
h_i/r_0	Reference	0.4	0.3	0.2	0.1	0.0	-0.1	-0.2	-0.3	-0.4
0.001	Present	8.3154	9.8002	11.3569	12.9848	14.6819	16.4468	18.2776	20.1731	22.1318
	[1]	8.3160	9.8008	11.3578	12.9855	14.6825	16.4472	18.2780	20.1734	22.1319
	[6]	8.2517	9.8171	11.3572	12.9829	14.6819	16.4574	18.3133	20.2322	22.2276
0.05	Present	8.3154	9.8002	11.3569	12.9848	14.6819	16.4468	18.2776	20.1731	22.1318
	[1]	8.2660	8.2660	11.2660	12.8660	14.5299	16.2557	18.0412	19.8844	21.7833
	[6]	8.3020	9.7487	11.2657	12.8636	14.5296	16.2661	18.0766	19.9432	21.8787
0.10	Present	8.3154	9.8002	11.3569	12.9848	14.6819	16.4468	18.2776	20.1731	22.1318
	[1]	8.1200	9.5320	10.9999	12.5208	14.0911	15.7076	17.3669	19.0658	20.8010
	[6]	8.1562	9.5488	11.0001	12.5186	14.0909	15.7178	17.4013	19.1233	20.8944
0.15	Present	8.3154	9.8002	11.3569	12.9848	14.6819	16.4468	18.2776	20.1731	22.1318
	[1]	7.8878	9.2163	10.5835	11.9849	13.4159	14.8719	16.3485	17.8414	19.3467
	[6]	7.9241	9.2333	10.5841	11.9830	13.4157	14.8818	16.3813	17.8970	19.4368

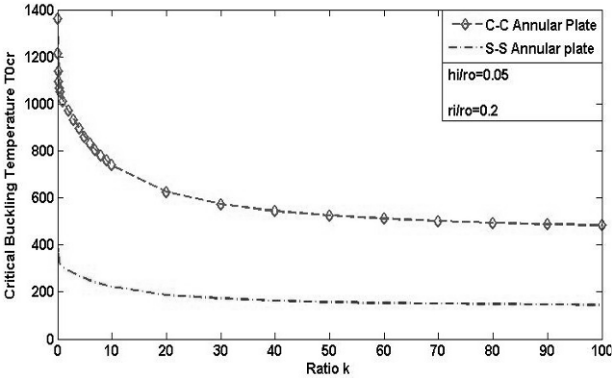

Fig. 7. Effect of volume fraction index, k, on the buckling temperature index T_{0cr} in uniform thickness annular plates for two kinds of supporting, C-C and S-S.

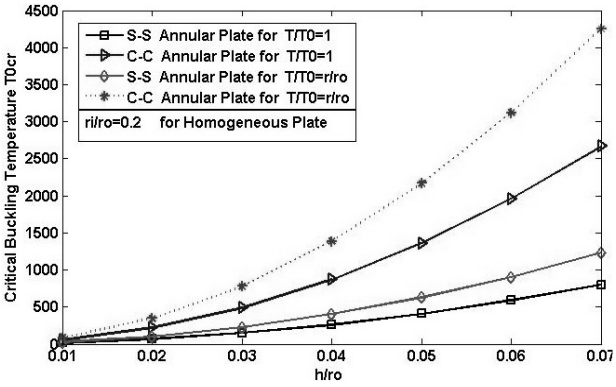

Fig. 8. Effect of h/r_o ratio on the buckling temperature index T_{0cr} in uniform thickness annular plates for two kinds of supporting, C-C, S-S.

Young's modulus is less than that of ceramic. This causes a decrease in T_{0cr}.

Effect of thickness to radius ratio, h/r_o, on T_{0cr} is investigated in Fig. 8, for two kinds of supporting, a C-C and a S-S, each one for two different types of temperature distributions, a uniform and a linear distribution. The annular plate is of uniform thickness, made fully of ceramic ($k = 0$), with $r_i/r_o = 0.2$. As seen in this figure, increasing h/r_o results in increase in T_{0cr} for all of the cases. Clamped plates have larger buckling temperature than simply supported plates under the same thermal load distribution. Also, the plates subjected to linear temperature distribution buckle at larger T_{0cr} than those which are under uniform temperature rise.

In Fig. 9 the buckling load factor λ_T is plotted versus the taper parameter, β, for linearly variable thickness FGM annular plates under three different types of temperature rise distributions, a uniform, a linear, and a parabolic distribution. As seen in this figure, for all three kinds of the temperature distributions, increasing β results in decrease in T_{0cr}.

Effect of the inner-to-outer-radius ratio, r_i/r_o, in the thermal buckling load factor of annular plates of uniform thickness is

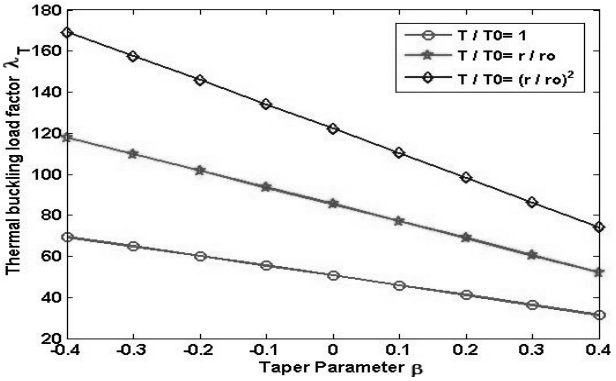

Fig. 9. Effect of taper parameter β on the buckling load factor λ_T of annular plates for uniform, linear, and parabolic temperature distribution.

investigated in Fig. 10, for 4 different types of edge supporting. In the plate with clamped supporting at both interior and exterior edges (C-C), and in the plate simply supported at the both edges (S-S), the thermal load factor λ_T increases with increase in r_i/r_o. For the two other supporting types, there are no serious

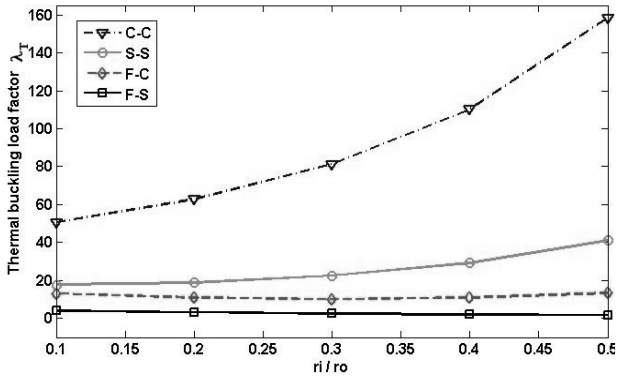

Fig. 10. Effect of r_i/r_o ratio on the thermal buckling load factor λ_T in uniform thickness annular plates for various kinds of edge supporting.

variations in λ_T. However, for the plate of F-C supporting, i.e. free at its interior edge and clamped at its exterior edge, λ_T decreases a little with increase in r_i/r_o, at interval r_i/r_o = [0.1 0.3], but at the remaining interval, i.e. r_i/r_o = [0.3 0.5], λ_T has inclined. For plate with F-S supporting, λ_T declines very slightly with increase in r_i/r_o at the whole interval.

In Figs. 11 and 12, the first mode shapes of buckling in homogenous circular and annular plates of linearly varying thickness are plotted for 3 different values of taper parameter, β. Mode shapes associated with circular plates having simply supported and clamped edges are shown in Figs. 11(a) and (b) respectively, and mode shapes of annular plates with S-S and C-C boundary conditions are depicted in Figs. 12(a) and (b) respectively. It is noticed that, in all of the cases, as the taper parameter increases, the plate maximum buckling deflection is shifted towards the exterior edge of the plate. This is in accordance with one's physical intuition, as for grater values of taper parameter the plate thickness and consequently the bending stiffness take smaller values at the points nearer to the exterior edges.

5. Concluding remarks

In this paper, a finite element formulation is derived for the thermal buckling behavior of axisymmetric FGM circular and annular plates of variable thickness, subjected to a temperature rise distribution that can be non-uniformly distributed along radial coordinate axis. The convergence of the FEM model is investigated, and also validated through comparison with references. Parametric studies are conducted, to investigate the effect of a number of important parameters which lead to the following deductions:

The value of the critical buckling temperature index, T_{0cr}, decreases as the volume fraction index, k, increments. In the plates of uniform thickness, increasing h/r_o results in increase in T_{0cr}. Clamped plates have larger buckling temperatures than their simply supported counterparts under the same temperature distribution. Plates under linear temperature distribution buckle at larger T_{0cr} than those subjected to uniform temperature rise. In tapered circular plates, λ_T decreases as β increases. In uniform thickness annular plates having C-C and S-S edge supports, λ_T increases as r_i/r_o increments in the interval [0.1 0.5]. However, for the plates with F-S and F-C supporting types, there are no serious variations in λ_T in the interval. In the first mode shape of buckling of circular and annular plates with linearly variable thicknesses having S-S and/or C-C supports, as the taper parameter increases, the plate maximum buckling deflection is shifted towards the exterior edge of the plate.

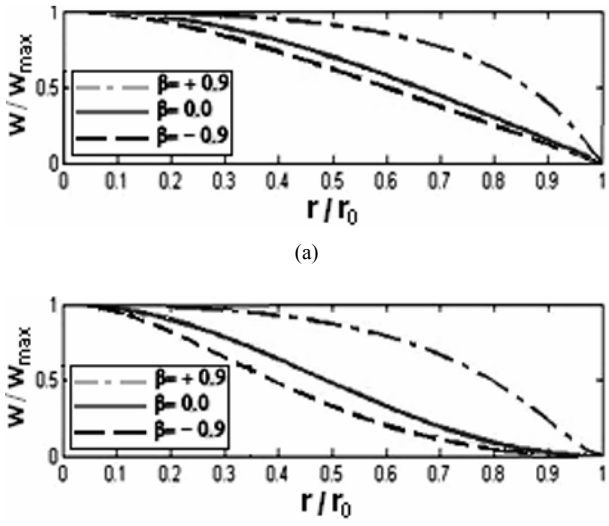

(a)

(b)

Fig. 11. First mode shape of buckling in tapered circular plates for 3 different values of β with (a) simply supported edges; (b) clamped edges.

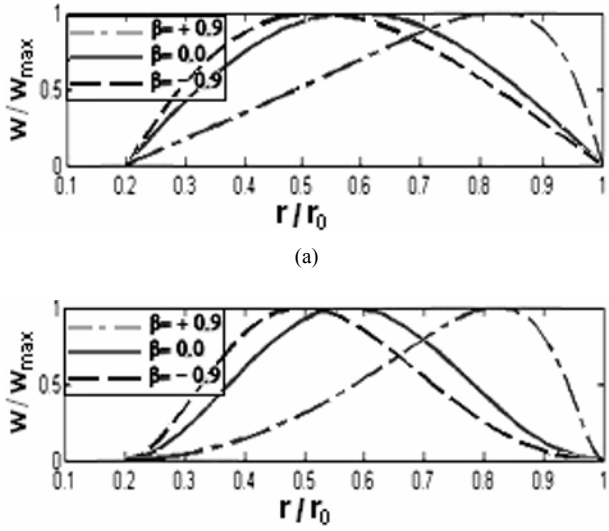

(a)

(b)

Fig. 12. First mode shape of buckling in tapered annular plates for 3 different values of β with (a) simply supported edges; (b) clamped edges.

Nomenclature

$[A]$	: Extensional stiffness matrix
D	: Plate flexural rigidity
E	: Elastic modulus
E_c, E_m	: Elastic modulus of ceramic and metal resp.
h_i, h_o	: Plate thicknesses at inner and outer edges resp.
k	: Volume fraction index
L	: Length of an element
M_r	: Mechanical moment resultant
N_r, N_θ	: Inplane mechanical force resultants
N_r^T, N_θ^T	: Inplane thermal force resultants
N_1^e, N_2^e	: Lagrangian shape functions
P	: A material property
P_c, P_m	: A material property of ceramic and metal resp.
r	: Radial coordinate
r_i, r_o	: Anular plate inner and outer radii resp.
T_0	: Temperature rise index
$T_{0\mathrm{cr}}$	: Critical value of the temperature index
U	: Strain energy stored in plate
u_0, w	: Midplate displacements along r and z coords.
V_r	: Effective lateral shear force resultant
W	: Work done by inplane forces due to buckling
z	: Coordinate through the plate thickness
α	: Coefficient of thermal expansion
α_c, α_m	: Coefficient of thermal expansion of ceramic and metal resp.
β	: Plate taper parameter
ΔT	: Temperature change
ε_r^0, ε_θ^0, $\gamma_{r\theta}^0$	: Midplane strains
η	: Degree of the thickness variations
$\kappa_r, \kappa_\theta, \kappa_{r\theta}$	: Plate curvatures
λ_T	: Thermal buckling load factor
ν	: Poisson's ratio
ξ	: Element local coordinate
σ_r, σ_θ, $\tau_{r\theta}$	: Stress components
$\phi_1^e, \phi_2^e, \phi_3^e, \phi_4^e$	: Hermitian shape functions

References

[1] K. K. Raju and G. V. Rao, Thermal post-buckling of linearly tapered moderately thick isotropic circular plates, *Comput Struct*, 58 (1996) 655-658.

[2] P. M. Ciancio and J. A. Reyes, Buckling of circular and annular plates of continuously variable thickness used as internal bulkheads in submersibles, *Ocean Engineering*, 30 (2003) 1323-1333.

[3] M. Özakça, N. Taysi and F. Kolcu, Buckling analysis and shape optimization of elastic variable thickness circular and annular plates—I. Finite element formulation, *Eng. Struct.*, 25 (2003) 181-192.

[4] M. M. Najafizadeh and B. Hedayati, Refined theory for thermoelastic stability of functionally graded circular plates, *Journal of thermal stresses*, 27:9 (2004) 857-880.

[5] E. Efraim and M. Eisenberger, Exact vibration analysis of variable thickness thick annular isotropic and FGM plates, *Journal of Sound and Vibration*, 299 (2007) 720-738.

[6] S. K. Jalali, M. H. Naei and A. Poorsolhjouy, Thermal stability analysis of circular functionally graded sandwich plates of variable thickness using pseudo-spectral method, *Materials and design*, 31 (2010) 4755-4763.

[7] A. M. Zenkour and M. Sobhy, Thermal buckling of various types of FGM sandwich plates, *Composite Structures*, 93-1 (2010) 93-102.

[8] A. C. Ugural, *Stresses in plates and shells*, 2nd ed., McGraw-Hill, Boston (1999).

[9] S. P. Timoshenko and J. M. Gere, *Theory of elastic stability,* 2nd ed., New York, McGraw-Hill (1961).

[10] J. N. Reddy, *An introduction to the finite element method*, 2nd ed., New York, McGraw-Hill (2005).

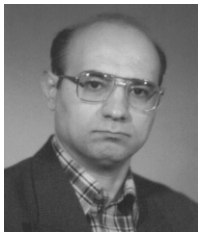

M. Mohieddin Ghomshei received his M.Sc. degree in Mechanical Engineering from Sharif University of Technology, Iran, in 1992 and his Ph.D. degree from Tehran University, Iran, in 2002. Dr. Ghomshei is currently an assistant professor at the department of mechanical engineering of Islamic Azad university-Karaj branch in Karaj, Iran. His research fields are mechanics of composite structures, and smart materials / structures.